Antireflective submicrometer gratings on thin-film silicon solar cells for light-absorption enhancement

Young Min Song,[1] Jae Su Yu,[2] and Yong Tak Lee[1,*]

[1]*Department of Information and Communications, Gwangju Institute of Science and Technology, 1 Oryong-dong, Buk-gu, Gwangju 500-712, Korea*

[2]*Department of Electrical Engineering, Kyung Hee University, 1 Seocheon-dong, Giheung-gu, Yongin-si, Gyeonggi-do 446-701, Korea*

**Corresponding author: ytlee@gist.ac.kr*

Received September 15, 2009; revised December 11, 2009; accepted December 12, 2009; posted December 23, 2009 (Doc. ID 117157); published January 21, 2010

This study reports highly efficient light-absorbing structures based on submicrometer gratings (SMGs) for thin-film crystalline silicon solar cells. The integration of SMGs into the cell structure leads to superior broadband antireflection properties compared to conventional antireflection coatings. With careful design optimization, an improvement of the cell efficiency of nearly 25.1% was obtained compared to double-layer coated solar cells. Optimized SMG structures were fabricated on a silicon substrate using interference lithography and a lenslike shape transfer process. The fabricated SMG structures exhibited low reflectivity in the wavelength range of 300–1200 nm, indicating good agreement with the simulated results. © 2010 Optical Society of America

OCIS codes: 050.6624, 040.5350, 260.2710.

Thin-film crystalline silicon (*c*-Si) solar cells are one of the promising candidates for low-cost photovoltaic applications because of commercially compatible mass-production processes. However, the relatively thin absorption region tends to degrade the cell efficiency, which is the main drawback of thin-film solar cells [1]. To improve light absorption in thin-film solar cells, it is mandatory to minimize the Fresnel reflection at the air/silicon interface in the range of the entire solar spectrum. Moreover, to achieve a high absorption efficiency for the entire day, an angle-independent antireflection property is required. Although multilayer antireflection coating is commonly used, it has problems related to material selection, thermal mismatch, and instability of the thin-film stacks [2]. Over the past decade, submicrometer grating (SMG) structures with a tapered feature have been focused on as a more practical method for ultrabroadband and omnidirectional antireflections [3–7]. While excellent antireflection properties of SMG structures have been demonstrated via reflectivity characterizations, there are few studies of SMG integrated solar cells [6,7]. In this Letter, thin-film *c*-Si solar cells integrated with SMGs are proposed for the enhancement of light absorption. The SMG structure is optimized toward a high cell efficiency using a rigorous coupled-wave analysis (RCWA) method. As a preliminary result, SMG structures were fabricated on silicon substrates, and their reflection properties were characterized in comparisons with theoretical simulation results using experimentally measured data.

The inset of Fig. 1 shows a schematic illustration of a 2 μm thin-film *c*-Si solar cell with SMGs. The SMG structures on the top surface of *c*-Si are used as an antireflective medium instead of single- and double-layer coatings. An aluminum (Al) metallic reflector is attached onto the rear side of the *c*-Si substrate for light trapping enhancement. To quantify the light-absorbing capability of the SMG structures, the RCWA method is used to calculate the reflectance and the absorption efficiency. The simulated model is assumed to be a closely packed truncated cone array with a period of 400 nm and a height of 400 nm. For comparison, we also calculated the reflectance of *c*-Si solar cells with a flat surface, a single-layer antireflection coating (ARC), and a double-layer ARC. Figure 1 shows the calculated reflectance spectra of thin-film *c*-Si solar cells with the Al metallic backreflector for different surface structures. For all surface structures, plots of the reflectance show smooth curves in the wavelength range below ~500 nm. This is similar to the reflectance of a bulk silicon substrate with both surface structures [8]. In the wavelength range above ~500 nm, however, ripple patterns occur owing to the interference of light reflected at the top surface and the *c*-Si/metal interface, which is analo-

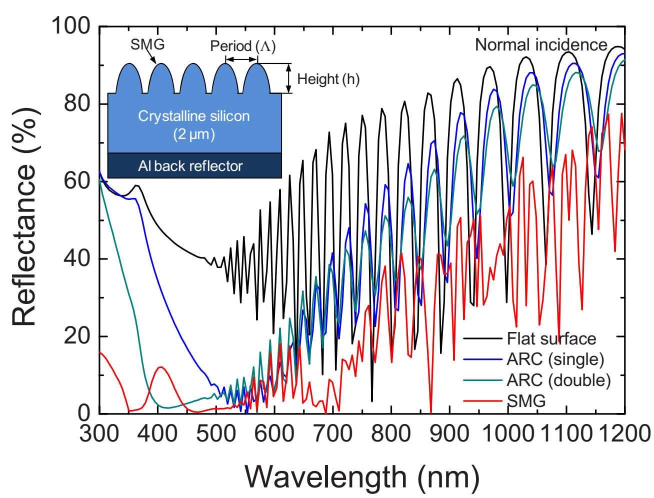

Fig. 1. (Color online) Calculated reflectance spectra of thin-film *c*-Si solar cells with the Al metallic backreflector for different surface structures. The inset shows schematic illustration of the thin-film silicon solar cell with SMGs.

0146-9592/10/030276-3/$15.00

gous to a Fabry–Perot etalon [9]. Despite these fluctuations, as shown in Fig. 1, it is clear that the SMG structure has broader antireflection regions compared to that of a single-layer or a double-layer ARC.

To maximize the absorption efficiency over a wide wavelength range, it is important to find the optimum period of the SMG structures. Figure 2(a) shows a contour plot of the variation of the absorption efficiency by the Si region as a function of the period and wavelength for a cone height of 400 nm. The absorption efficiency is decreased as the period increases at a shorter wavelength, while it is increased at a longer wavelength. These phenomena can be explained by the fact that the reflection minima are shifted toward a higher wavelength region as the period of the SMGs increases [10]. From Fig. 2(a), it is possible to estimate that the optimal period is approximately 400 nm, providing a relatively high absorption efficiency in the visible (VIS) and near-infrared (NIR) wavelength regions. For a quantitative analysis, the solar cell efficiency was calculated using the equation $\eta = J_{sc} V_{oc} \Gamma_f / P_{in}$ [11,12], where J_{sc} is the short-circuit current density, V_{oc} is the open-circuit voltage, Γ_f is the filling factor, and P_{in} is the total incident power under the AM1.5 solar spectrum. In our calculation, the collection efficiency of 85% with a 5% shadowing effect from the electrode was used. The reverse bias saturation current was taken to be 1.5×10^{-15} A/cm^2, and the filling factor was fixed to 80%. The details of the procedure used can be found in the literature [12]. Figure 2(b) shows the calculated cell efficiency of thin-film *c*-Si solar cells with SMGs versus a cone period with 2, 5, and 8 μm cell thicknesses. The calculated cell efficiency of the SMG integrated solar cells has higher values than that of the reference double ARC solar cells (11.53%) in the period range of 100–800 nm. As expected from Fig. 2(a), the cell efficiency of the 2 μm thick SMG solar cells has a maximum value at a period of 400 nm. The maximum cell efficiencies of the 2-, 5-, and 8-μm-thick solar cells were 14.36%, 18.44%, and 20.42%, respectively, corresponding to a period of 400 nm. This indicates that the optimal period is not dependent on the cell thickness.

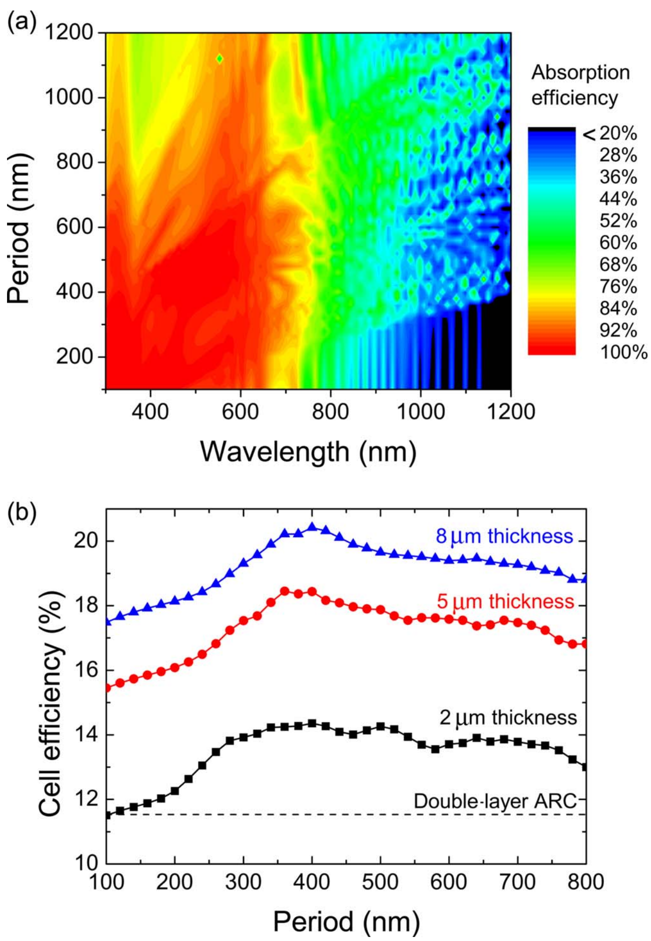

Fig. 2. (Color online) (a) Contour plot of the variation of absorption efficiency as a function of period and wavelength for a 400 nm cone height. (b) Calculated cell efficiency of thin-film *c*-Si solar cells with SMGs versus the cone period for 2, 5, and 8 μm cell thicknesses.

To analyze the effect of varying the height of the SMG structures on the cell efficiency, further simulations were performed. Figure 3 shows a contour map of the cell efficiency of the SMG integrated thin-film *c*-Si solar cells as a function of the cone period and height. At small heights, the cell efficiency is relatively low over the entire period range as the effective refractive index appears abrupt to the incoming light. As the height is increased, the cell efficiency is enhanced and the region with a high cell efficiency become broadens. In practical solar cell applications, however, it is clear that a taller cone requires complex process steps, which increases the fabrication cost. Therefore, the cone height and period should be carefully chosen according to this contour map. As shown in Fig. 3, SMG structures with a period of 400 nm and a height of 400 nm exhibit a higher cell efficiency in a reasonable process range.

To verify the validity of the silicon SMG structures, SMG structures were fabricated with a period of 400 nm and a height of 400 nm on silicon substrates as a preliminary result of SMG *c*-Si solar cells. For the fabrication of the SMGs, the pattern transfer of a lenslike-shaped photoresist formed by a thermal reflow process was used together with interference lithography using a 363.8 nm argon laser [5]. The inset

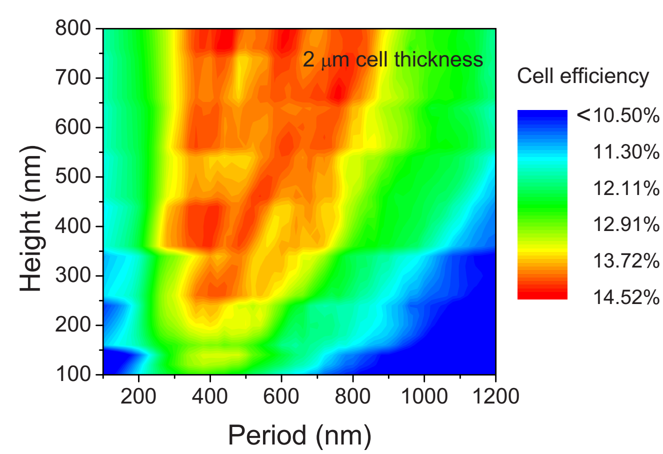

Fig. 3. (Color online) Contour map for the cell efficiency of the SMG integrated thin-film *c*-Si solar cells as a function of the cone period and height.

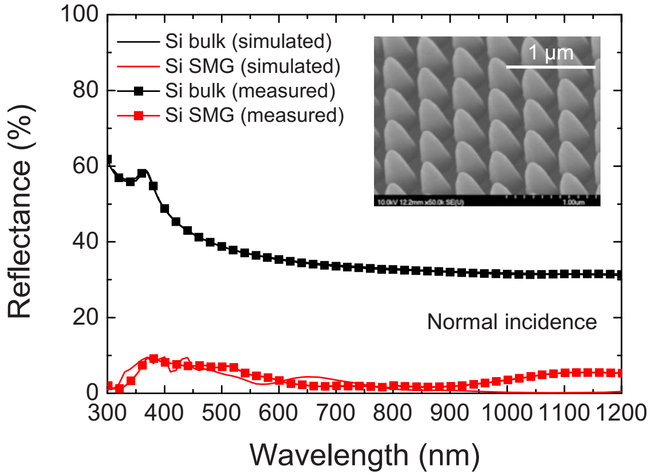

Fig. 4. (Color online) Measured and simulated reflectance as a function of wavelength for the bulk silicon and the fabricated silicon SMG structure. The inset shows the SEM image of the fabricated silicon SMG structures with 400 nm period and 400 nm height.

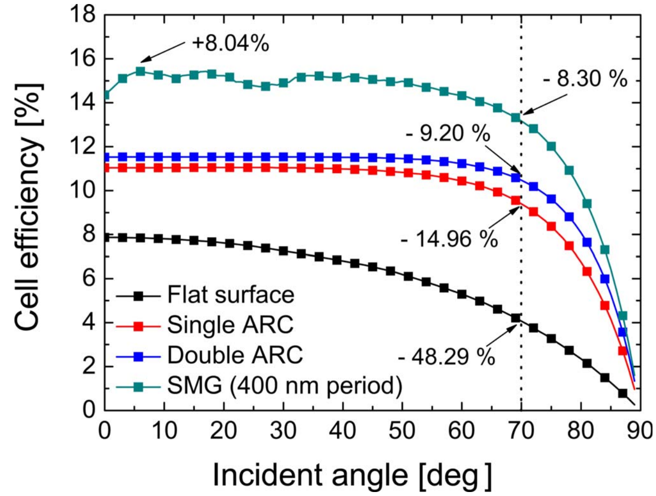

Fig. 5. (Color online) Cell efficiency of the 2-μm-thick *c*-Si solar cells with four different surface structures as a function of incident angle. The period and height of SMG structures are both 400 nm.

of Fig. 4 shows a scanning electron microscope (SEM) image of the silicon SMG structures fabricated with a period of 400 nm and a height of 400 nm. The fabricated SMG structures consist of tapered grating arrays, resulting in a graded index profile. The reflectance of the fabricated silicon SMG structures was measured at normal incidence using a UV-VIS-NIR spectrophotometer and was also calculated by the RCWA method. As shown in Fig. 4, the measured reflectance values of the silicon SMG structures are significantly reduced compared to the bulk silicon, and the values are in good agreement with the calculated values.

The influence of the incident angle of light on the efficiency of a solar cell is crucial for the device performance. Figure 5 shows the cell efficiency of the 2-μm-thick *c*-Si solar cells with four different surface structures as a function of the incident angle. The cell efficiency of *c*-Si solar cells with a flat surface drops rapidly as the incident angle increases due to the increased reflection loss as shown in Fig. 5. In the SMG integrated solar cells, however, the cell efficiency is sustained at an incident angle in excess of 60°, and it is degraded by only 8.3% at 70° compared to that at 0°. This angle-independent optical property is required for the device to operate efficiently by day and night. More interestingly, the device exhibits a better performance at a slightly tilted incident angle compared with the normal incidence angle. This efficiency enhancement is attributable to the extended optical path length [12].

In summary, SMG integrated thin-film *c*-Si solar cells that can be used to enhance the absorption efficiency over a wide wavelength range and for a wide angle of the incident light are presented. The preliminary SMG structures fabricated by simple process steps on a silicon substrate exhibit a reflectance of less than 10% in 300–1200 nm range, which is in good agreement with the simulation results. This proposed structure is expected to be an effective approach for increasing the cell efficiency for realizing high-efficiency, low-cost, thin-film *c*-Si solar cells.

This work was partially supported by the IT R&D program of The Ministry of Knowledge Economy/The Institute of Information Technology Advancement (2007-F-045-03) and by the Research Institute for Solar and Sustainable Energies (RISE), GIST.

References

1. M. A. Green, K. Emery, Y. Hishikawa, and W. Warta, Prog. Photovoltaics **16**, 61 (2008).
2. P. Lalanne and G. M. Morris, Proc. SPIE **2776**, 300 (1996).
3. Y. Kanamori, M. Sasaki, and K. Hane, Opt. Lett. **24**, 1422 (1999).
4. C. C. Striemer and P. M. Fauchet, Appl. Phys. Lett. **81**, 2980 (2002).
5. Y. M. Song, S. Y. Bae, J. S. Yu, and Y. T. Lee, Opt. Lett. **34**, 1702 (2009).
6. H. Sai, H. Fujii, K. Arafune, Y. Ohshita, Y. Kanamori, H. Yugami, and M. Yamaguchi, Jpn. J. Appl. Phys. Part 1 **46**, 3333 (2007).
7. H. Sai, Y. Kanamori, K. Arafune, Y. Ohshita, and M. Yamaguchi, Prog. Photovoltaics **15**, 415 (2007).
8. S. Chhajed, M. F. Schubert, J. K. Kim, and E. F. Schubert, Appl. Phys. Lett. **93**, 251108 (2008).
9. P. G. O'Brien, N. P. Kherani, A. Chutinan, G. A. Ozin, S. John, and S. Zukotynski, Adv. Mater. **20**, 1577 (2008).
10. S. A. Boden and D. M. Bagnall, Appl. Phys. Lett. **93**, 133108 (2008).
11. S. M. Sze, *Physics of Semiconductor Devices*, 2nd ed. (Wiley, 1981), Chap. 14.
12. N. N. Feng, J. Michel, L. Zeng, J. Liu, C.-Y. Hong, L. C. Kimerling, and X. Duan, IEEE Trans. Electron Devices **54**, 1926 (2007).